Enhancing Exoskeleton Assistance Flow Control by Leveraging Human Variability and Probabilistic Movement Primitives

Aymeric Orhan, Duy Hoàng, Olivier Bruneau, Bastien Berret, Franck Geffard

Enhancing Exoskeleton Assistance Flow Control by Leveraging Human Variability and Probabilistic Movement Primitives

Aymeric Orhan [1,2*], Duy Hoàng [2,3], Olivier Bruneau [1], Bastien Berret [4], Franck Geffard [2]

[1]LURPA, Mechanical Engineering Department, ENS Paris-Saclay, Université Paris-Saclay, Gif-sur-Yvette, 91190, France.
[2]CEA, List, Université Paris-Saclay, Palaiseau, 91120, France.
[3]Université de Versailles Saint-Quentin-en-Yvelines, Université Paris-Saclay, Versailles, 78035, France.
[4]CIAMS, Université Paris-Saclay, Inria, Gif-sur-Yvette, 91190, France.

*Corresponding author(s). E-mail(s): orhanaymeric@gmail.com;

Abstract

Exoskeletons have the potential to significantly reduce users' physical effort and decrease the risk of work-related musculoskeletal disorders by providing robotic assistance. Human motor control is governed by a complex interaction between the central nervous system, the musculoskeletal system and the environment, generally leading to relatively fast, precise, smooth, and efficient movements. As a result, designing exoskeletons that provide assistance without being perceived as disruptive is challenging; they must be capable of predicting and adapting smoothly to the user's intended movements. In this paper, we propose leveraging the inherent variability in human movement to enhance the acceptability and comfort of upper-limb exoskeleton assistance. For that purpose, we use demonstrations from the human user and an online prediction method to infer their trajectory continuously, and we use an adaptive flow controller to adjust the assistance accordingly. We then increase the level of guidance and reduce correctivity of the exoskeleton when the users normally exhibit high variability, taking advantage of the higher tolerance to deviations from the planned trajectory in these phases to provide a stronger guidance while accommodating these deviations with higher compliance. Our approach was tested with the ABLE7D upper-limb exoskeleton during reaching tasks. The results demonstrate that our

method can effectively reduce the user's physical effort, notably by lowering muscle co-contractions, compared to a classical data-based solution, while providing a comfortable level of assistance.

1 Introduction

Exoskeletons have emerged as a promising solution for assisting human movement, offering significant benefits across a range of applications, from rehabilitation and medical support [1] to workplace ergonomics and enhanced physical performance [2], [3]. By providing targeted support to specific joints or muscle groups, exoskeletons can reduce the physical strain, mitigate the risk of musculoskeletal disorders, and improve overall user endurance [4]. However, despite these advantages, achieving seamless integration between an exoskeleton and its user is a significant challenge [5]. For an exoskeleton to be truly effective, it must not only assist movement but do so in a manner that feels natural and unobtrusive to the user [6].

A common approach to tackle this problem is to leverage physiological recordings of the users to predict his intent. Using technology such as electroencephalography (EEG) [7], electromyography (EMG) [8], or gaze [9], has allowed the detection of human motion intent at a high level. However, these classification methods typically yield only high-level intents, such as the desired direction or target of movement, which are insufficient for optimizing the exoskeleton's assistance throughout the entire motion. Conversely, when the upcoming trajectory is not predetermined (unlike in [10], [11]), its prediction is often carried out by regressing from continuous EMG measurements [12], [13], or from kinematic data, as it is commonly done in learning-by-demonstration (LbD) approaches [14], [15].

In this study we use such an LbD approach, namely Probabilitic Movement Primitives (ProMPs) [16]. This method stems from the idea of Movement Primitives [17]. This theory posits that complex movements are executed by combining motion primitives, i.e. synchronizing and modulating simpler actions [18]. ProMPs enable the encoding of joint coupling, temporal scaling and include a representation of variability in their formulation. ProMPs have already been applied to robotic upper-limb assistance in the work of [19] with a velocity-based Flow Controller (FC) based on the work of [20]. This FC defines a flow field around a reference trajectory, that is in this case the movement prediction.

Robotic assistance around a reference trajectory for physical human-robot interaction is a common approach that has been used in many exoskeleton control strategies [21]–[28]. This FC approach introduced by [20] applies corrective torques matching a viscous force in the direction of the flow field built around the reference trajectory. It has been shown that this approach can effectively guide the user while being less resistive to deviations than previous attempts (e.g., [29], [30]) with a lower-limb exoskeleton and path control approaches. The work in [19] extended the approach to an upper-limb

exoskeleton and showed that updating the reference trajectory online using ProMPs can effectively help provide a more comfortable interaction. Our approach follows these lines but seeks to improve the FC by tuning its parameters according to the human movement characteristics. In particular, an assistive robot should be more compliant to deviations around the reference trajectory when the variability of natural human movement is large [31], along with accommodating this characteristic, we also increase the guidance of the assistance in these high variability regions to leverage the natural high tolerance to deviations from the planned trajectory of the user.

In this paper, we thus leverage the information on variability issued from ProMPs to modulate the flow field and assistive force of the FC. Therefore, the variability of the user's demonstrations is exploited to enhance the trade-off between guidance and correction throughout the motion. To evaluate our approach we conducted an experimental study with the upper-limb ABLE exoskeleton to assist participants in a reaching task. We compared the performance of our assistance (henceforth denoted as VIFC, for Variability Informed FC) with the original FC design in [19], using target and user-specific experimental data (denoted as OFC, for Original FC). We collected motion-related information including EMG measurement of the elbow's and shoulder's flexor and extensor muscles and the exoskeleton's kinematics. Additionally, we gathered the qualitative feedback from the users with a questionnaire and a NASA-TLX survey [32]. Using these measurements, we show that adapting a robotic assistance according to human motion variability information can help to provide a more comfortable interaction.

2 Materials and Methods

2.1 Trajectory prediction

The reference trajectory around which the assistance is built must represent the user intent as best as possible so that the interaction between the user and the exoskeleton is as seamless as possible. As mentioned in the introduction we used ProMPs [16] to obtain prediction of upcoming movements that we can use as reference trajectory.

ProMPs is a data-based method that can learn a distribution over discrete-time trajectories [16]. It is data-based in the sense that demonstrations are needed in order to learn such a distribution. Then, predictions about the upcoming trajectory can be obtained at low computational cost by conditioning the distribution with an observation. In this section we introduce the ProMPs framework as defined by [16], expressed in discrete time for 2 joints as in [33].

1) Temporal scaling : To achieve temporal modulation or scaling, a phase variable $\tau(t)$ is introduced. This parameter can be set as any function monotically increasing with t [16]. In this paper, we defined $\tau(t) = \frac{t}{T}$, with T the final timestep. We simplify the phase dependency notation for any function in the following fashion: $\tau := \tau(t)$. This temporal scaling is inherent to ProMPs formulation, necessary to ensure a correct encoding of time-related characteristics in the space of representation of the method (the weights vectors space).

2) Encoding trajectories: The method of ProMPs encodes trajectories using basis functions. Here we used Gaussian functions $b_{i,t} = \exp(-\frac{(\tau - c_i)^2}{2\mathrm{l}_i})$ with c_i the i-th Gaussian basis function center parameter and l_i the i-th Gaussian basis function width parameter for the i-th basis function. These functions are classically used for point-to-point movements in a joint-level formulation [16]. We define the i-th basis function for a joint j position at timestep t as:

$$ {}^{i}\phi_{j,t} = \frac{b_{i,t}}{\sum_{k=1}^{n_{\mathrm{bf}}} b_{k,t}} \tag{1} $$

For our usage of these functions each width l_i is set as a constant: $\mathrm{l}_i = \mathrm{l} = -\frac{1}{8{n_{\mathrm{bf}}}^2 \log(\mathrm{o})}$, where o is an overlap parameter set to $\mathrm{o} = 0.7$ and n_{bf} is the number of basis functions (set to 30 in this study as in [19], a choice motivated as it allows good reconstruction precision while being computationally efficient). Similarly, we set each c_i so that functions are uniformally distributed along an extension of the phase domain $[-2\mathrm{l}; 1 + 2\mathrm{l}]$, i.e. $c_{i+1} - c_i = 1/n_{\mathrm{bf}}$ (for $i < n_{\mathrm{bf}}$) as in [34].

The n_{bf}-dimensional vector $\boldsymbol{\phi}_{j,t}$ is defined as the concatenation of these basis functions: $\boldsymbol{\phi}_{j,t} = [{}^{1}\phi_{j,t}, \ldots, {}^{n_{\mathrm{bf}}}\phi_{j,t}]$. We then define the corresponding basis function matrix for a joint j position and velocity at timestep t as $\boldsymbol{\Phi}_{j,t} = [\boldsymbol{\phi}_{j,t}, \dot{\boldsymbol{\phi}}_{j,t}] \in \mathbb{R}^{n_{\mathrm{bf}} \times 2}$ and the block diagonal matrix of basis function $\boldsymbol{\Psi}_t = \mathrm{blkdiag}(\boldsymbol{\Phi}_{1,t}^\top, \boldsymbol{\Phi}_{2,t}^\top) \in \mathbb{R}^{4 \times 2n_{\mathrm{bf}}}$ defined for both joints. We can extend this matrix to include all time steps by vertical concatenation as $\boldsymbol{\Psi}_{0:T} = [\boldsymbol{\Psi}_0^\top \cdots \boldsymbol{\Psi}_T^\top]^\top \in \mathbb{R}^{4(T+1) \times 2n_{\mathrm{bf}}}$. Let us define the arm joint position and velocity as $\boldsymbol{\Gamma}_t = [q_{1,t}, \dot{q}_{1,t}, q_{2,t}, \dot{q}_{2,t}]^\top \in \mathbb{R}^4$. The full trajectory can be represented through vertical concatenation as the vector $\boldsymbol{\Gamma}_{0:T} = [\boldsymbol{\Gamma}_0^\top \cdots \boldsymbol{\Gamma}_T^\top]^\top \in \mathbb{R}^{4(T+1)}$. Then, the trajectory of the 2-dof arm can be completely represented via a $2n_{\mathrm{bf}}$-dimensional weight vector $\boldsymbol{w} \in \mathbb{R}^{2n_{\mathrm{bf}}}$. This representation is given at each time step by the relation:

$$ \boldsymbol{\Gamma}_t = \boldsymbol{\Psi}_t \boldsymbol{w} + \boldsymbol{\epsilon}_\Gamma \tag{2} $$

with $\boldsymbol{\epsilon}_\Gamma \sim \mathcal{N}(0, \boldsymbol{\Sigma}_\Gamma)$ i.i.d Gaussian noise.

The probability of observing a trajectory $\boldsymbol{\Gamma}_{0:T}$ can then be expressed using the weight vector $\boldsymbol{w}$:

$$ p(\boldsymbol{\Gamma}_{0:T} | \boldsymbol{w}) = \prod_{t=0}^{T} \mathcal{N}(\boldsymbol{\Gamma}_t | \boldsymbol{\Psi}_t \boldsymbol{w}, \boldsymbol{\Sigma}_\Gamma). \tag{3} $$

To determine the weight vector in this framework from one demonstrated trajectory, we can use a regression method. In this work we used the ordinary least square (OLS) method as in [19], here written for the trajectory $\boldsymbol{\Gamma}_{0:T}$:

$$ \boldsymbol{w} = (\boldsymbol{\Psi}_{0:T}^\top \boldsymbol{\Psi}_{0:T} + \lambda \boldsymbol{I})^{-1} \boldsymbol{\Psi}_{0:T}^\top \boldsymbol{\Gamma}_{0:T} \tag{4} $$

with $\lambda = 10^{-2}$ a regularization parameter taken from [19].

The variability of human movement is captured by expressing the weight vector $\boldsymbol{w}$ as a Gaussian distribution $p(\boldsymbol{w}; \boldsymbol{\mu}_w, \boldsymbol{\Sigma}_w)$. Then, the mean and covariance parameters

can be estimated from several demonstrations as follows:

$$\begin{aligned}\boldsymbol{\mu}_w &= \frac{1}{M}\sum_{i=1}^{M}\boldsymbol{w}_i, \\ \boldsymbol{\Sigma}_w &= \frac{1}{M-1}\sum_{i=1}^{M}(\boldsymbol{w}_i-\boldsymbol{\mu}_w)(\boldsymbol{w}_i-\boldsymbol{\mu}_w)^\top\end{aligned} \tag{5}$$

where M is the number of demonstrations and $\boldsymbol{w}_i$ is the weight computed for the i^{th} trajectory using equation (4).

3) Inferring a trajectory from an observation: Once the distribution $p(\boldsymbol{w};\boldsymbol{\mu}_w,\boldsymbol{\Sigma}_w)$ has been learned from demonstrations, it can be used to infer trajectory. Let $\boldsymbol{\Lambda}_t^{\text{obs}} = \{\boldsymbol{\Gamma}_t^{\text{obs}},\boldsymbol{\Sigma}_\Gamma^{\text{obs}}\}$ denote an observation of a partial movement. We can use Bayes theorem on the learned theorem with this observation so as to condition the distribution in the following fashion: $p(\boldsymbol{w}|\boldsymbol{\Lambda}_t^{\text{obs}}) \propto \mathcal{N}(\boldsymbol{\Gamma}_t^{\text{obs}}|\boldsymbol{\Psi}_t\boldsymbol{w},\boldsymbol{\Sigma}_\Gamma^{\text{obs}})p(\boldsymbol{w})$. This conditioned distribution of $\boldsymbol{w}$ by $\boldsymbol{\Lambda}_t^{\text{obs}}$ is Gaussian and given by the following mean and covariance:

$$\begin{aligned}\hat{\boldsymbol{\mu}}_w &= \boldsymbol{\mu}_w + \boldsymbol{\Sigma}_w\boldsymbol{\Psi}_t^\top\boldsymbol{S}_t(\boldsymbol{\Gamma}_t^{\text{obs}}-\boldsymbol{\Psi}_t\boldsymbol{\mu}_w), \\ \hat{\boldsymbol{\Sigma}}_w &= \boldsymbol{\Sigma}_w - \boldsymbol{\Sigma}_w\boldsymbol{\Psi}_t^\top\boldsymbol{S}_t\boldsymbol{\Psi}_t\boldsymbol{\Sigma}_w\end{aligned} \tag{6}$$

where $\boldsymbol{S}_t = (\boldsymbol{\Sigma}_\Gamma^{\text{obs}} + \boldsymbol{\Psi}_t\boldsymbol{\Sigma}_w\boldsymbol{\Psi}_t^\top)^{-1}$.

The prediction $\boldsymbol{\Gamma}_{0:T}^{\text{pred}}$ can then be computed by weighting the basis functions with the mean of this conditioned distribution:

$$\boldsymbol{\Gamma}_{0:T}^{\text{pred}} = \boldsymbol{\Psi}_{0:T}\hat{\boldsymbol{\mu}}_w. \tag{7}$$

During the assistive trials the prediction was updated at a frequency of 20Hz for the first 40% of the trajectories as in [19]. After 40% of the trajectory, the prediction is generally accurate enough for the rest of the trajectory and stopping the trajectory update results in a better task success likelihood. This threshold is estimated with phase τ as described in 2.2. Fig. 1 shows typical prediction adjustement during an assistive trial.

2.2 Flow Controller

Our controller design is derived from the FC presented in [19], [20]. This controller defines the assistance from a flow field that is shaped from a reference trajectory. We used the same formulation as in [19], [20], but used variability information to dynamically adjust the FC during the movement execution, as proposed/described below.

Let us denote the current position in the cartesian space as $\mathbf{p}_{c,t} = [y_t, z_t]$ at timestep $t \in \{0, 1, ..., N\}$ during a trajectory. The reference trajectory is obtained using the ProMPs prediction as introduced in 2.1. The reference position $\mathbf{p}_{ref,t}$ corresponding to $\mathbf{p}_{c,t}$ is then defined as the closest point to the current position in the cartesian space on the reference trajectory. The corresponding phase is thus taken for

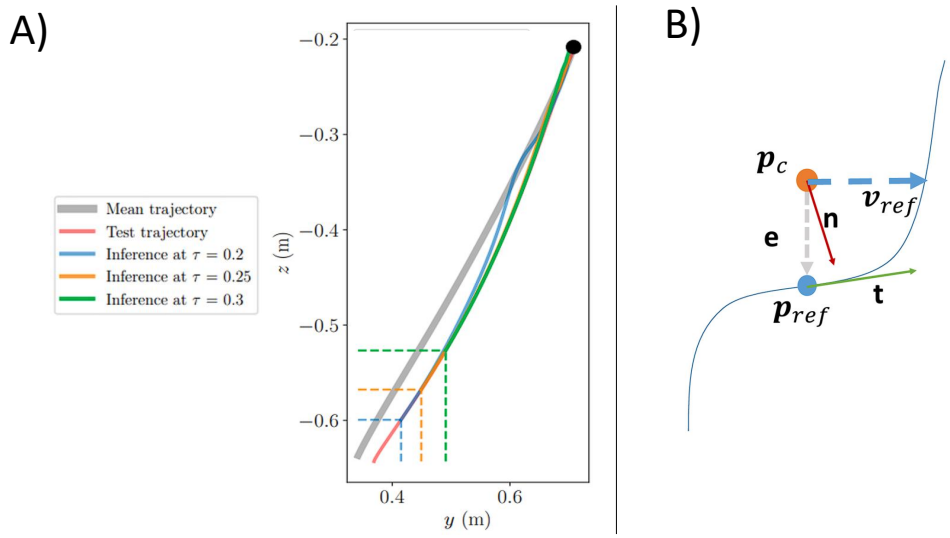

Fig. 1 panel A: trajectory prediction online updating during the movement with ProMPs. Panel B: depiction of the vectors for an abstract trajectory used to define the flow field as detailed in II.B.

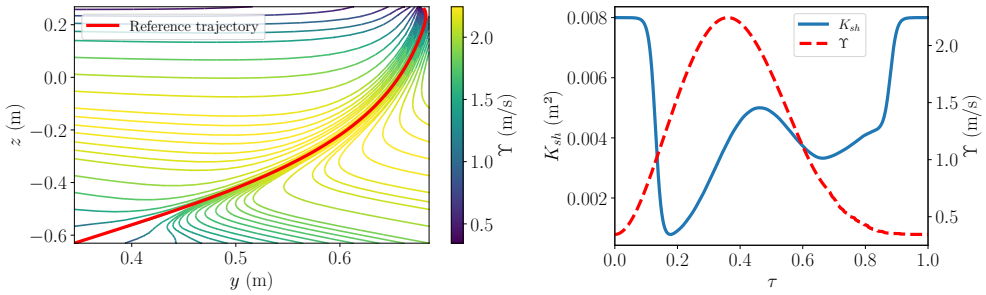

Fig. 2 Left panel: Flow field representation for target 4 (T_4) with our proposed improvement. The controller compliance in the early and late phase of the movement can be clearly observed. Note that the field is modified during the assistance due to the updating of the reference trajectory using the predictions. Right Panel: K_{sh} and Υ modulation along the phase of the movement for T_4.

current phase of the movement. For this section we alleviate the notation with the following for all dependence to the timestep: $y_t = y$. And the error vector is defined with $\mathbf{e} = \mathbf{p}_{ref} - \mathbf{p}_c$.

The normalized tangent $\mathbf{t}$ and normal $\mathbf{n}$ vectors at point $\mathbf{p}_{ref}$ of the current ProMP distribution, are respectively denoted $\mathbf{t}$ and $\mathbf{n}$. This tangent vector and the normal vector to the reference trajectory $\mathbf{n}$ at $\mathbf{p}_{ref}$ are used to define a normal vector to the

reference trajectory pointing towards the reference trajectory $\hat{\mathbf{n}}$ when placed at $\mathbf{p}_c$:

$$\hat{\mathbf{n}} = \begin{cases} -\mathbf{n} \text{ if } \theta < 90^\circ \\ \mathbf{n} \quad \text{else} \end{cases} \tag{8}$$

where θ is the angle between $\mathbf{e}$ and the normal to the curve. A representation of these vector is given in Fig. 1.

The equation of the flow field is then defined as a compromise between a tangential and normal component, i.e. a guiding and a corrective component using these vectors, the speed at the current position of the flow field is expressed with $\mathbf{v}_{ref}$:

$$\mathbf{v}_{ref} = \begin{cases} \Upsilon \frac{(|e|\hat{\mathbf{n}} + \frac{K_{sh}}{|e|}\mathbf{t})}{|(|e|\hat{\mathbf{n}} + \frac{K_{sh}}{|e|}\mathbf{t})|} & \text{for } |e| \geq 1e^{-5} \\ \Upsilon \mathbf{t} & \text{for } |e| < 1e^{-5} \end{cases} \tag{9}$$

where Υ and K_{sh} are two scalars defining respectively the magnitude of the velocity and the compromise between the guiding and corrective repartition of the assistance along the tangential and normal vector previously defined. The guidance imposed by the field corresponds to $\mathbf{v}_{ref}$ along the $\mathbf{t}$ vector, and the correction to $\mathbf{v}_{ref}$ along $\hat{\mathbf{n}}$. Note that both are conditioned by the magnitude of the field Υ.

Our contribution to the design of the FC consists in dynamically modifying the controller parameters Υ and K_{sh} along the phase of the movement according to velocity profiles and human variability information obtained from demonstrations encoded in ProMPs.

The parameter K_{sh} is inversely proportional to the correctiveness of the controller. When K_{sh} is high, the assistance is slightly corrective whereas if K_{sh} is low, the assistance is highly corrective. We posit that when variability is high we can increase the guidance and magnitude of our assistance (resulting in a decrease of correctiveness) as the user will be more likely to accept deviations from the planned trajectory that the stronger assistance may create.

Precisely we define K_{sh} using two empirical constants. These values, M_{var} and m_{var} correspond respectively to the maximum and the minimum of standard deviation measured from the demonstrations. Similarly, we denote v as the standard deviation value at the current phase of the ProMPs encoded demonstration dataset. Note that this value is constant throughout trials towards the same target at the same phases as it is independent of trajectory predictions updates. Using the updated ProMPs distribution's variance to define this parameter would entail an undesirable and erroneous bias of this value as the variability of the conditioned distribution is null at the conditioned points. We then define K_{sh} as a remapping of these values between chosen K_{sh} bounds: $[5e^{-3}, 5e^{-2}]$ (in m^2):

$$K_{sh} = 5e^{-3} + \frac{4.5e^{-2}(v - m_{var})}{M_{var} - m_{var}} \tag{10}$$

However this definition can lead to highly corrective assistance at the start and end of the movement which can lead to high resistance for the user if its actual intent

and our prediction diverge. To counter this effect we set K_{sh} equal to $8e^{-2}\,m^2$ when the phase is lower than 0.1 or higher than 0.9. This way 10% of the movement at the beginning and at the end is hard-coded to ensure a compliant assistance to user intent. Fuzzy logic functions are used to smoothly transition out and in of those regions. Fig. 2 shows how K_{sh} typically behaves during a movement and the ensuing effect on the flow field definition.

The parameter Υ corresponds directly to the magnitude of the flow field's reference velocity as defined by equation (9). More concretely, Υ defines the exoskeleton's hand target velocity value. In this work, the preferred human velocity is considered at each motion phase rather than the maximum value of velocity to modulate our assistance. Using $\hat{V}_k$ and V_t^M, which represent respectively the mean and maximum velocity observed at the current timestep of the movement in the demonstrations to define Υ. Υ is then computed at the timestep $t \in [0, N]$ with the following equation:

$$\Upsilon_t = \hat{V}_t + \frac{1}{N+1}\sum_{k=0}^{N}(V_k^M - \hat{V}_k) \tag{11}$$

The first component of equation (11) mimics the mean behavior of the user while the second component ensures the assistive capacity of the robot since the reference velocity is always greater than the human velocity.

Once the flow field is defined, the assistive force of the exoskeleton is set as the force applied by a viscous fluid on an immersed symmetric body due to drag:

$$\mathbf{F}_a = C_{drag}(\mathbf{v}_{ref} - \mathbf{v}_c) \tag{12}$$

where $\mathbf{v}_c$ is the current hand velocity vector, estimated with the exoskeleton's incremental encoders and C_{drag} is the drag coefficient set equal to 20Ns/m as in [19]. The assistive force $\mathbf{F}_a$ was updated at a frequency of 1Khz for all conditions.

In the original FC formulated in [19], a 250ms waiting period after movement onset is used before activation of the assistance in an attempt to not disturb the movement. Our modulation of Υ and K_{sh} allowed us to eliminate this waiting period in our proposed improvement while still offering a compliant albeit low assistance in the beginning of the movement.

The online implementation of our method was successfully implemented at a frequency of 1 kHz for both prediction and assistance calculations, indicating real-time capability. We set the prediction update at a 20 Hz rate, a choice similar to [19] made to ensure responsive but stable assistive behaviour as updating the reference trajectory at a higher frequency could lead to an over compliant assistance with no task success guarantee as the assistive force will always be tangent to the movement.

2.3 Experimental Design

To evaluate the performance of our variability informed FC an experiment has been conducted with 11 participants. In the following section the experimental design and protocol are described.

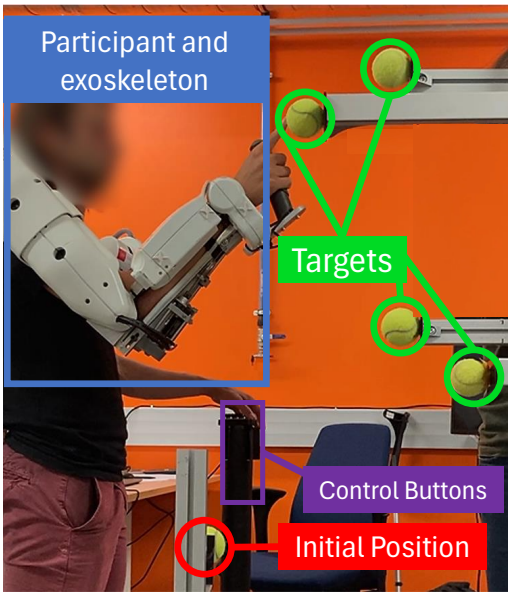

Fig. 3 Experimental setup. Participants started their reaching movements at the initial position to a given target, starting the assistance with the control buttons. Note that in this picture T_1 was slided backwards to free the workspace for reaching movements toward T_4.

Task The experiment was divided into 3 blocks. During the first block participants were asked to perform 15 reaching movements towards targets in front of them as shown in Fig. 3 (four targets denoted as T_1, T_2, T_3 and T_4). The demonstrations obtained were then used to train ProMPs distribution for each target and used for predicting upcoming movements as explained in 2.1. The 2 other blocks were conducted in a random order for each participants. They consisted of performing the same reaching movements with an assistance defined using the OFC or the VIFC. Directly after each of these blocks we collected the participants qualitative results using a survey, described in section III.A, and a NASA-TLX questionnaire. Participants remained unaware of the nature and of which assistive mode they were evaluating until the experiment was completely finished.

Participants Eleven healthy young adults (3 Female) participated in the experiment. The participants, with a mean age of 29.91 ± 2.39 years, mean height of 1.75 ± 0.1m, and mean weight of 67.09 ± 12.27kg, were right-handed adults without any known neurological disorders or injuries that could have affected the experiment. Written informed consent was obtained from all participants in accordance with the Helsinki declaration, and the protocol was approved by the local ethical committee for research.

Data Collection. The reaching task was performed while wearing a backdrivable robotic exoskeleton for the upper limb (ABLE, [35], [36]). This exoskeleton features seven active joints, three replicating the human gleno-humeral joint, one emulating human elbow flexion/extension and three recreating the radiocarpal joint. Movements were measured using the internal encoders of the exoskeleton worn by participants

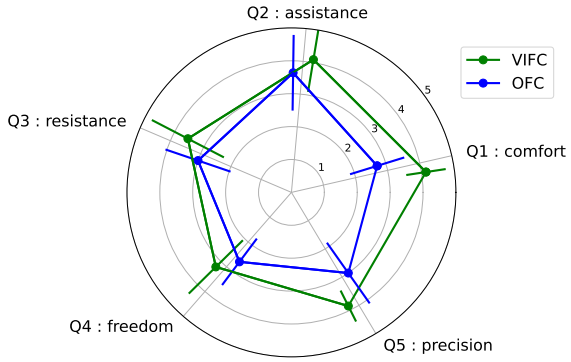

Fig. 4 Qualitative results to the questionnaire (mean+std for each question).

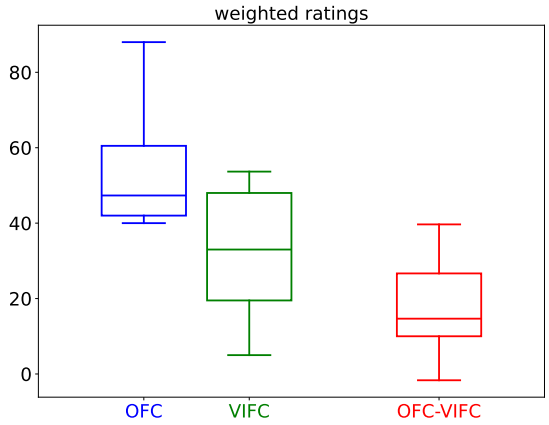

Fig. 5 Qualitative results to the NASA-TLX survey (weighted ratings and relative difference between those ratings). The relatively large variance in results concerning the NASA TLX likely stems from the large variability of biologic profiles in participants. Note that the difference between these two ratings (OFC - VIFC) is always positive, indicating that VIFC was always perceived as better than OFC.

at a frequency of 1 kHz. We measured the EMG signals of 6 muscles responsible for shoulder and elbow flexion and extension: the posterior and anterior deltoids, the lateral and long-head triceps, the bicep and the bracho-radialis. The EMG sensors were placed according to the SENIAM recommendations [37].

3 Results

3.1 Qualitative Results

Participant's subjective feedback on each assistive mode was measured using a Likert-scale of 5 items, from strongly disagree (0) to strongly agree (5). Five statements were evaluated by participants:

- Q1: Achieving the task was comfortable.
- Q2: The exoskeleton assisted me in accomplishing the task.
- Q3: The exoskeleton did not resist my movement.
- Q4: I felt free to execute my movement as I wanted to.
- Q5: I could accurately reach the target.

As stated in section II.C we additionally estimated the physical exertion of participants after each experimental block using a NASA TLX questionnaire. To limit desirability bias [38], participants were asked to give an immediate answer and that there was no right or wrong answer, they could also give us written or additional remarks. Furthermore, the experiment occurred in full anonymity. This questionnaire has been used in the field exoskeleton upper-limb assistance [39] and as such allows comparisons with other control mode in the literature. This questionnaire is more relevant to our field and provides a clearer impression of the interaction of the user with the exoskeleton than the NASA-TLX survey. Nevertheless we still provide NASA-TLX results to enhance comparability of our results with other control modes as it is a more standard qualitative feedback survey.

Result to the Likert-scale questionnaire are shown in Fig. 4. A statistical analysis was conducted and statistical significance ($p < 0.05$). A Shapiro-Wilk [40] test was first realized and revealed that the data distribution was not normal after which we conducted a Wilcoxon-Nemenyi test on each question for each assistive mode to assess significance. Statistical significance between improved and original control mode was established for all questions.

Similarly, a statistical analysis was conducted with the same procedure for the NASA TLX weighted ratings results, shown in Fig. 5. Statistical significance was established between our proposed VIFC: 33.18 ± 16.11 and the baseline OFC: 52.82 ± 14.45 controller modes ($p < 0.001$). We posit that the relatively large variance in results concerning the NASA TLX stems from the large variability of biologic profiles from participants (ranging from 1m53 to 1m95). Note that all participants followed the same trend in grading the VIFC systematically lower than the OFC: the difference between OFC-VIFC was systematically positive ($= 19.6 \pm 16.3$ mean and std).

3.2 Quantitative Results

Table 1 shows the results of the Wilcoxon-Nemenyi pairwise test (conducted after a Shapiro-Wilk test confirmed non normal distributions) on different evaluated parameters, including the peak velocity (PV), peak acceleration (PA), motion duration (MD), root-mean-square of the assistive force (F_a RMS) measured using the exoskeleton's encoders. And the muscle activation (MA) and muscle co-contraction index (CCI)

measured using EMGs (see **Data Collection** in section 2.3). The notations SF, SE, EF, and EE relate to the activation of corresponding muscles: shoulder flexor, shoulder extensor, elbow flexor, and elbow extensor.

Table 1 Results of Wilcoxon-Nemenyi pairwise comparisons (Trans for Transparent mode)

Parameter		OFC vs VIFC	OFC vs Trans	VIFC vs Trans
PV		$p > 0.05$	$\mathbf{p < 0.001}$	$\mathbf{p < 0.001}$
PA		$p > 0.05$	$\mathbf{p < 0.001}$	$\mathbf{p < 0.001}$
MD		$p > 0.05$	$\mathbf{p < 0.01}$	$\mathbf{p < 0.01}$
F_a RMS		$\mathbf{p < 0.001}$		
MA	SF	$p > 0.05$		
	SE	$p > 0.05$		
	EF	$\mathbf{p < 0.01}$		
	EE	$\mathbf{p < 0.001}$		
CCI	Shoulder	$\mathbf{p < 0.05}$	$\mathbf{p < 0.01}$	$\mathbf{p < 0.01}$
	Elbow	$\mathbf{p < 0.001}$	$p > 0.05$	$p > 0.05$

Impact on movement kinematics. A strong modification of movement kinematics was observed, as can be seen in Fig. 6 and Fig. 8. This is expected since the target speed of our assistance is higher than the mean natural speed of the participant's demonstrations due to the definition of the Υ parameter in the FC design. Consequently, the duration of movements, shown in Fig. 7, was also impacted and we observe a statistically significant difference between the transparent and the assistive modes. We also show the RMS of assistive force from the exoskeleton for each control mode in Fig. 7.

Muscle activation and co-contraction. The difference in movement duration and speed between the transparent and assistive modes makes the comparison of muscle activation with EMG signals hard to perform as shown in [41], [42]. However, EMG signals can be used to compare the impact of each assistive mode on muscle activation as movement duration and speed variations across these are not statistically significant (according to Wilcoxon-Nemenyi test between OFC and VIFC in PV and MD). We show in Fig. 9 the muscle activation results for the assistive modes.

Statistical analysis was conducted to report significant differences between control conditions in elbow muscle activation. In both elbow flexor and extensor, the OFC induced significantly more muscle activity than our VIFC ($p < 0.01$).

We computed a co-contraction index as defined in [43]. The results for this index for the elbow and shoulder across all participants and assistive mode are shown in Fig. 10. We conducted a statistical analysis that established a significant reduction of muscle co-contraction for both joints using the VIFC. We observed a statistically significant increase between the transparent mode and the assistive modes for the shoulder but not for the elbow. All statistical analyses are reported in table 1.

3.3 Discussion

We show that considering, and modulating accordingly the assistance, with human movement variability is effective. Precisely, our global strategy provides a stronger and

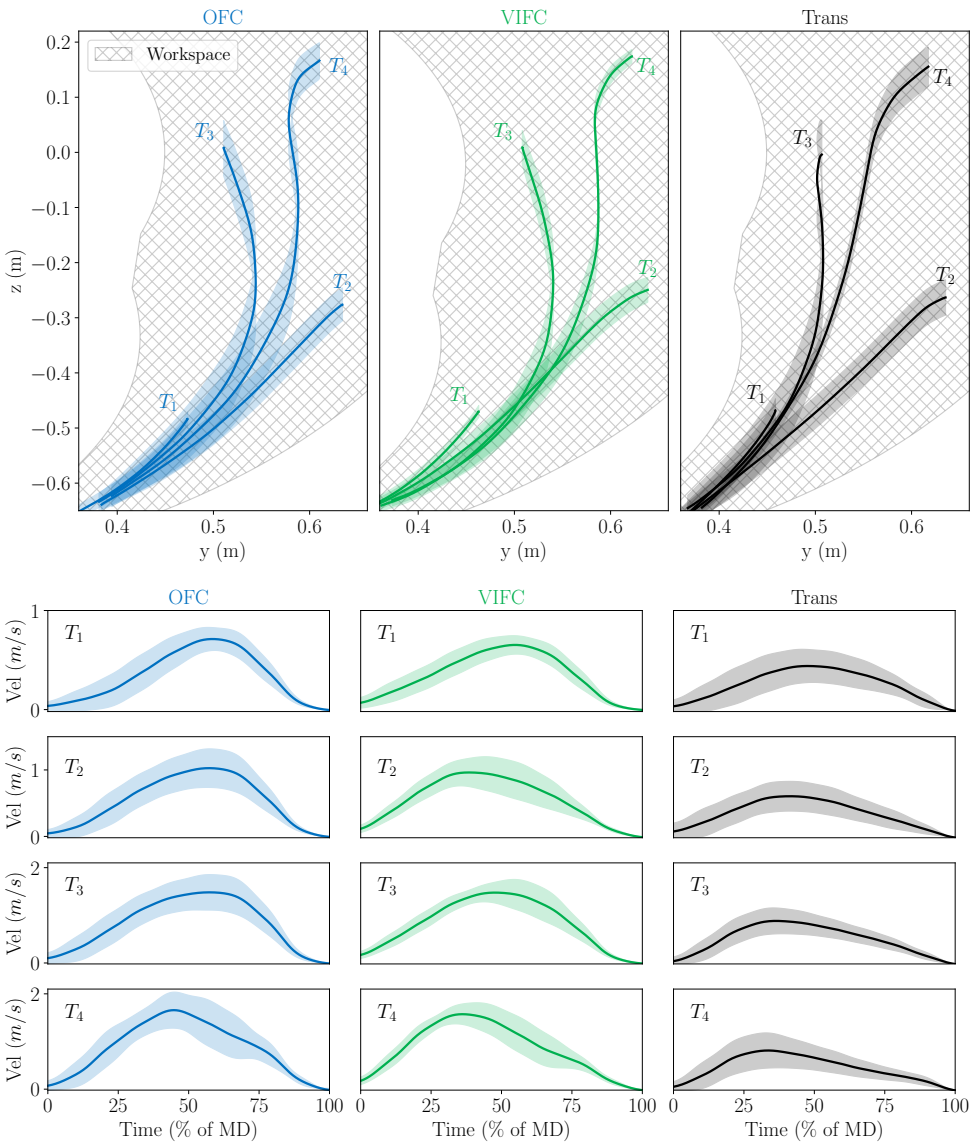

Fig. 6 Left panel: cartesian movements for each target and assistive condition, including transparent (Trans) mode, across all participants. Right Panel: Velocity profiles for all targets across all participants. Mean and std in plain line and shaded area respectively for both figures.

less corrective assistance in high variability regions of the movement. Both quantitative and qualitative results show that such a strategy enables a more seamless interaction, minimizing the exoskeleton's resistance by better incorporating the user's habits and acting accordingly. Although the assistive force of the exoskeleton (see Fig. 7) is lower

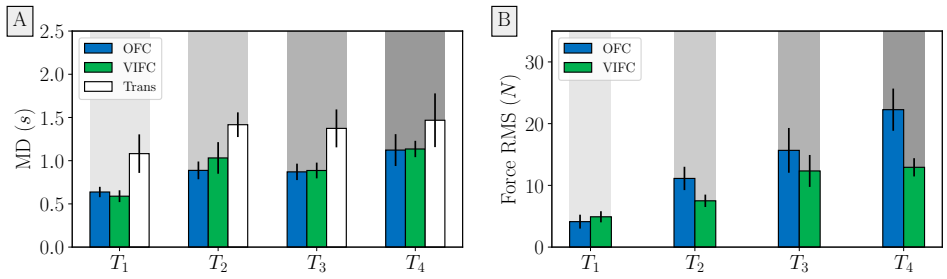

Fig. 7 Left panel: Movement duration. Right Panel: Assistive force. Both metrics for all assistive conditions and transparent (Trans) mode as well for movement duration, for the four targets across all participants.

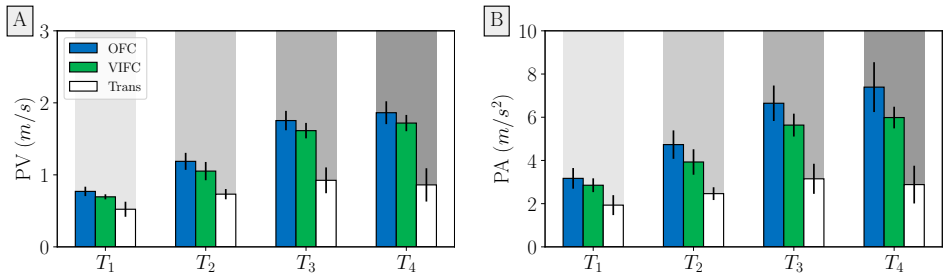

Fig. 8 Peak velocity (panel A) and peak acceleration (panel B) for all assistive condition and transparent mode. Note a clear augmentation for all assistive mode compared to the transparent (Trans) mode.

with this modulation, we believe that this avoided the adverse effects of the assistance that previously led to higher stiffness in the user. Indeed we can see from the reduction of muscle activation in Fig. 9 and muscle co-contraction in Fig. 10 that we were able to prevent these effects.

Although we have shown that our variability-informed design can provide a more comfortable interaction than a classical approach, it still needs to be compared with other types of assistance such as gravitational support [44], [45] or bilateral interactive control such as differential game theory [11], [46], [47]. However the idea of modulating the assistance according to user variability may be applied to these methods as well, and help create a more comfortable interaction.

One could argue that a more longitudinal study is necessary to establish our claim as users could learn to better use the exoskeleton and achieve the best use of each control mode. Despite our experiment occurring in a 2-hour span, to assess this idea we ensured a large volume of movements for each participant (60 in total) and a familiarization period with the exoskeleton and evaluated any learning curve appearance in our performance metrics (mainly EMGs recordings but kinematics as well). We report no such phenomenon of user learning in our context, which could indicate that

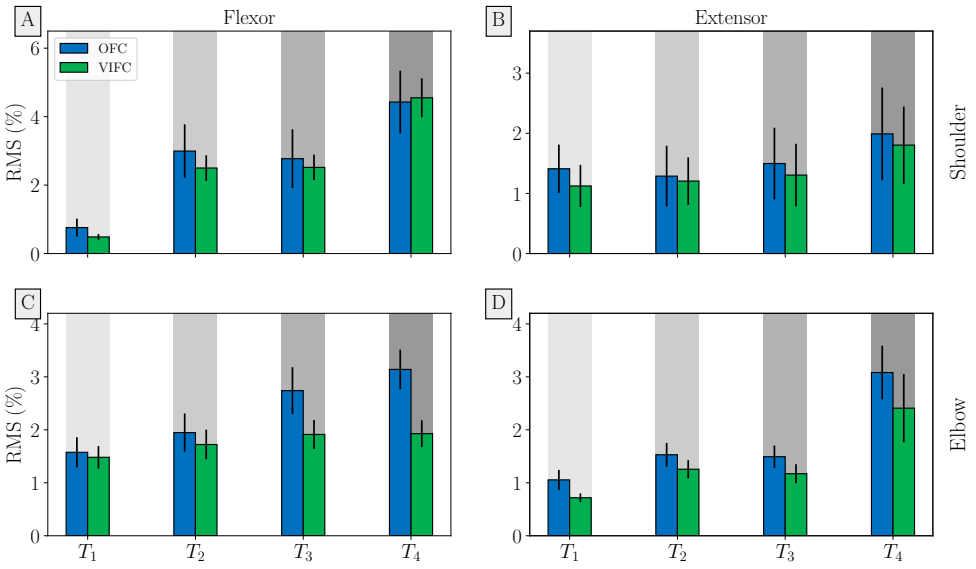

Fig. 9 Measured muscle activation for the shoulder and elbow flexor and extensor muscles across all participants. We do not show muscle activation in transparent mode as that comparison is largely biased by the difference in movement durations as shown in [41], [42]. Note that the decrease in effort is apparent in the Elbow joint, and specifically the elbow flexor. This may be due to the nature of the movements in the experimental procedure as elbow flexion was the main required motion with the most amplitude.

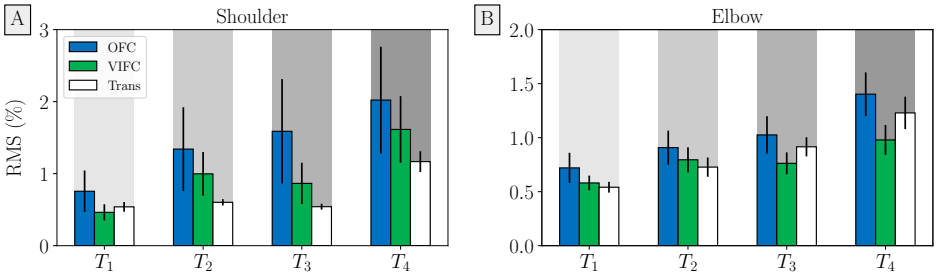

Fig. 10 Measured co-contraction of the shoulder and elbow muscles for all assistive condition and transparent mode across all participants.

the assistive mode is intuitive and natural enough for an immediate adaptation and learning.

Additionally, our method still needs to be tested on a more diverse set of movements with more complex contexts, as our task was limited to reaching movements, a choice motivated to provide a controlled setting that allows for clear measurement of movement variability and muscle activation, critical for assessing the feasibility of our adaptive control approach.

4 Conclusion

Recent advances in upper-limb exoskeleton control have focused on non-invasive methods for predicting human motion intents. When the absence of bio-information limits prediction accuracy, effective assistance has been achieved in repetitive tasks using demonstrated movements [19], [20], [24], [29], [30], [48], [49]. Interestingly, some of the developed techniques also incorporate information on the variability of the human user's movements [19], [50]. Building on these insights, our study leveraged this variability to modulate the assistance of an upper-limb exoskeleton using a velocity flow controller as suggested by [19]. Our findings provide empirical evidence that incorporating this factor can lead to a more seamless interaction between the user and the exoskeleton, reducing adversarial effects of robotic assistance, as demonstrated by a decrease in muscle co-contraction.

However, these types of approaches are still constraining in many regards, mainly due to their lack of generality and the necessary training period. Whereas these drawbacks could perhaps be acceptable in a rehabilitation setting, they are crucial to limit for an actual use in an industrial setting.

Recently, the work of [33] suggested using artificial demonstrations instead of real demonstrated trajectories from the user for the training of the LbD method (here ProMPs). As it could help palliate a drawback of our assistance, further work could investigate the possibility of replacing the real distribution of arm trajectories with artificial human-like ones with our VIFC design in a future study.

Further work could extend our approach to situations where the controller is not informed about which particular target the user wants to reach, so as to increase the usability and generality of our approach. In this case, one could use classification strategies that have been recently developed using ProMPs [50] to infer the user's goal and associated trajectory. Additionally, recent advances in phase estimation with ProMPs [51] could be integrated to our work as we modulate and compute the assistance according to this phase, which is then a critical factor.

While the work of [19] highlighted the gains of continuously updating the prediction at a 20Hz frequency, our more intricate shaping of the flow field leads to a different situation. If this shape definition is sufficiently precise, it may help reduce the necessity of continuous trajectory predictions altogether, as the gain in compliance shifts from trajectory updates with predictions to compliant field definition, meaning that our method could decrease the rate at which the reference trajectory is updated. However the adaptability to a new target exhibited by [19] remains desirable. The recent work in [33] shows that this adaptability is restricted to targets sufficiently close to the learned target as the prediction error increases with target distance and that other strategies are necessary for these targets, such as artificial demonstrations from a model-based approach.

Overall our approach can help create a better interaction between the exoskeleton and the user while providing an efficient assistance. We believe that the idea of adapting assistance to the variability of human movement can help provide a better interaction and is exportable to other assistive methods.

5 Statements and Declarations

5.1 Funding.

This work is supported in part by the French National Agency for Research (grant ANR-19-CE33-0009)

5.2 Competing Interests.

The authors have no relevant financial or non-financial interests to disclose.

5.3 Authors Contributions.

All authors contributed to the study conception and design. Material preparation, data collection and analysis were performed by Orhan Aymeric and Hoàng Duy. The first draft of the manuscript was written by Orhan Aymeric and all authors commented on previous versions of the manuscript. All authors read and approved the final manuscript.

5.4 Data Availability.

Data sets generated during the current study are available from the corresponding author on reasonable request.

5.5 Ethics Approval.

As stated in section 2.3, written informed consent was obtained from all participants in accordance with the Helsinki declaration, and the protocol was approved by the local ethical committee for research. The authors affirm that human research participant provided informed consent for publication of Fig.3.

References

[1] T. Proietti, V. Crocher, A. Roby-Brami, and N. Jarrasse, "Upper-Limb Robotic Exoskeletons for Neurorehabilitation: A Review on Control Strategies," *IEEE reviews in biomedical engineering*, vol. 9, pp. 4–14, 2016, ISSN: 1941-1189. DOI: 10.1109/RBME.2016.2552201.

[2] M. A. Nussbaum, B. D. Lowe, M. de Looze, C. Harris-Adamson, and M. Smets, "An Introduction to the Special Issue on Occupational Exoskeletons," *IISE Transactions on Occupational Ergonomics and Human Factors*, vol. 7, no. 3-4, pp. 153–162, Oct. 2019, ISSN: 2472-5838. DOI: 10.1080/24725838.2019.1709695.

[3] L. Lang, J. Xiao, Y. Sun, H. Lu, Z. Zhou, and C. Yang, "Scale Force Control of an Exoskeleton for Human Performance Augmentation," *Journal of Intelligent & Robotic Systems*, vol. 106, no. 1, p. 22, Sep. 2022, ISSN: 1573-0409. DOI: 10.1007/s10846-022-01611-6.

[4] G. Bao, L. Pan, H. Fang, *et al.*, "Academic Review and Perspectives on Robotic Exoskeletons," *IEEE transactions on neural systems and rehabilitation engineering: a publication of the IEEE Engineering in Medicine and Biology Society*, vol. 27, no. 11, pp. 2294–2304, Nov. 2019, ISSN: 1558-0210. DOI: 10.1109/TNSRE.2019.2944655.

[5] F. Safavi, P. Olikkal, D. Pei, *et al.*, "Emerging Frontiers in Human–Robot Interaction," *Journal of Intelligent & Robotic Systems*, vol. 110, no. 2, p. 45, Mar. 2024, ISSN: 1573-0409. DOI: 10.1007/s10846-024-02074-7.

[6] Y. Li, A. Sena, Z. Wang, *et al.*, "A review on interaction control for contact robots through intent detection," *Progress in Biomedical Engineering*, vol. 4, Jul. 2022. DOI: 10.1088/2516-1091/ac8193.

[7] C. Huang, Y. Xiao, and G. Xu, "Predicting Human Intention-Behavior Through EEG Signal Analysis Using Multi-Scale CNN," *IEEE/ACM transactions on computational biology and bioinformatics*, vol. 18, no. 5, pp. 1722–1729, 2021, ISSN: 1557-9964. DOI: 10.1109/TCBB.2020.3039834.

[8] E. Trigili, L. Grazi, S. Crea, *et al.*, "Detection of movement onset using EMG signals for upper-limb exoskeletons in reaching tasks," *Journal of NeuroEngineering and Rehabilitation*, vol. 16, no. 1, p. 45, Mar. 2019, ISSN: 1743-0003. DOI: 10.1186/s12984-019-0512-1.

[9] H. Admoni and S. Srinivasa, "Predicting User Intent Through Eye Gaze for Shared Autonomy," in *AAAI Fall Symposia*, 2016.

[10] T. Teramae, T. Noda, and J. Morimoto, "EMG-Based Model Predictive Control for Physical Human–Robot Interaction: Application for Assist-As-Needed Control," *IEEE Robotics and Automation Letters*, vol. 3, no. 1, pp. 210–217, Jan. 2018, ISSN: 2377-3766. DOI: 10.1109/LRA.2017.2737478.

[11] A. Hafs, D. Verdel, W. Gomes, O. Bruneau, and B. Berret, "Optimizing human-robot interactions through differential game control," in *Workshop on Multilimb Coordination in Human Neuroscience and Robotics: Classical and Learning Perspectives, IROS*, 2023.

[12] L. Bi, A. Feleke, and C. Guan, "A review on EMG-based motor intention prediction of continuous human upper limb motion for human-robot collaboration," *Biomedical Signal Processing and Control*, vol. 51, pp. 113–127, May 2019. DOI: 10.1016/j.bspc.2019.02.011.

[13] L. Quesada, D. Verdel, O. Bruneau, B. Berret, M.-A. Amorim, and N. Vignais, *EMG-to-torque Models for Exoskeleton Assistance: A Framework for the Evaluation of in Situ Calibration*. Jan. 2024. DOI: 10.1101/2024.01.11.575155.

[14] S. Calinon, F. D'halluin, E. L. Sauser, D. G. Caldwell, and A. G. Billard, "Learning and Reproduction of Gestures by Imitation," *IEEE Robotics & Automation Magazine*, vol. 17, no. 2, pp. 44–54, Jun. 2010, ISSN: 1558-223X. DOI: 10.1109/MRA.2010.936947.

[15] Z. Yu, J. Zhao, D. Chen, S. Chen, and X. Wang, "Adaptive Gait Trajectory and Event Prediction of Lower Limb Exoskeletons for Various Terrains Using Reinforcement Learning," *Journal of Intelligent & Robotic Systems*, vol. 109, no. 2, p. 23, Sep. 2023, ISSN: 1573-0409. DOI: 10.1007/s10846-023-01963-7.

[16] A. Paraschos, C. Daniel, J. R. Peters, and G. Neumann, "Probabilistic Movement Primitives," p. 9, 2013.

[17] F. A. Mussa-Ivaldi, "Modular features of motor control and learning," *Current Opinion in Neurobiology*, vol. 9, no. 6, pp. 713–717, 1999, ISSN: 1873-6882. DOI: 10.1016/S0959-4388(99)00029-X.

[18] T. Flash and B. Hochner, "Motor primitives in vertebrates and invertebrates," *Current Opinion in Neurobiology*, vol. 15, no. 6, pp. 660–666, Dec. 2005, ISSN: 0959-4388. DOI: 10.1016/j.conb.2005.10.011.

[19] M. Jamšek, T. Kunavar, U. Bobek, E. Rueckert, and J. Babič, "Predictive Exoskeleton Control for Arm-Motion Augmentation Based on Probabilistic Movement Primitives Combined With a Flow Controller," *IEEE Robotics and Automation Letters*, vol. 6, no. 3, pp. 4417–4424, Jul. 2021, ISSN: 2377-3766. DOI: 10.1109/LRA.2021.3068892.

[20] A. Martinez, B. Lawson, C. Durrough, and M. Goldfarb, "A Velocity-Field-Based Controller for Assisting Leg Movement During Walking With a Bilateral Hip and Knee Lower Limb Exoskeleton," *IEEE Transactions on Robotics*, vol. 35, no. 2, pp. 307–316, Apr. 2019, ISSN: 1552-3098, 1941-0468. DOI: 10.1109/TRO.2018.2883819.

[21] N. Hogan, "Impedance Control: An Approach to Manipulation: Part II—Implementation," *Journal of Dynamic Systems, Measurement, and Control*, vol. 107, no. 1, pp. 8–16, Mar. 1985, ISSN: 0022-0434. DOI: 10.1115/1.3140713.

[22] N. Hogan, "Impedance Control: An Approach to Manipulation: Part I—Theory," *Journal of Dynamic Systems, Measurement, and Control*, vol. 107, no. 1, pp. 1–7, Mar. 1985, ISSN: 0022-0434, 1528-9028. DOI: 10.1115/1.3140702.

[23] G. Aguirre-Ollinger, J. E. Colgate, M. A. Peshkin, and A. Goswami, "Active-Impedance Control of a Lower-Limb Assistive Exoskeleton," in *2007 IEEE 10th International Conference on Rehabilitation Robotics*, Jun. 2007, pp. 188–195. DOI: 10.1109/ICORR.2007.4428426.

[24] F. Müller, J. Jäkel, and J. Suchy, "Tunnel-shaped potential force fields for improved hand-guiding of robotic arms," in *2015 20th International Conference on Methods and Models in Automation and Robotics (MMAR)*, Aug. 2015, pp. 429–434. DOI: 10.1109/MMAR.2015.7283914.

[25] H. T. Tran, H. Cheng, H. Rui, X. Lin, M. K. Duong, and Q. Chen, "Evaluation of a Fuzzy-Based Impedance Control Strategy on a Powered Lower Exoskeleton," *International Journal of Social Robotics*, vol. 8, no. 1, pp. 103–123, Jan. 2016, ISSN: 1875-4805. DOI: 10.1007/s12369-015-0324-9.

[26] S. Y. A. Mounis, N. Z. Azlan, and F. Sado, "Assist-as-needed control strategy for upper-limb rehabilitation based on subject's functional ability," *Measurement and Control*, vol. 52, no. 9-10, pp. 1354–1361, Nov. 2019, ISSN: 0020-2940. DOI: 10.1177/0020294019866844.

[27] R. Cao, L. Cheng, C. Yang, and Z. Dong, "Iterative assist-as-needed control with interaction factor for rehabilitation robots," *Science China Technological Sciences*, vol. 64, no. 4, pp. 836–846, Apr. 2021, ISSN: 1869-1900. DOI: 10.1007/s11431-020-1671-6.

[28] Y. Guo, H. Wang, Y. Tian, and D. G. Caldwell, "Task performance-based adaptive velocity assist-as-needed control for an upper limb exoskeleton," *Biomedical Signal Processing and Control*, vol. 73, p. 103 474, Mar. 2022, ISSN: 1746-8094. DOI: 10.1016/j.bspc.2021.103474.

[29] S. K. Banala, S. H. Kim, S. K. Agrawal, and J. P. Scholz, "Robot Assisted Gait Training With Active Leg Exoskeleton (ALEX)," *IEEE Transactions on Neural Systems and Rehabilitation Engineering*, vol. 17, no. 1, pp. 2–8, Feb. 2009, ISSN: 1558-0210. DOI: 10.1109/TNSRE.2008.2008280.

[30] A. Duschau-Wicke, J. von Zitzewitz, A. Caprez, L. Lunenburger, and R. Riener, "Path control: A method for patient-cooperative robot-aided gait rehabilitation," *IEEE transactions on neural systems and rehabilitation engineering: a publication of the IEEE Engineering in Medicine and Biology Society*, vol. 18, no. 1, pp. 38–48, Feb. 2010, ISSN: 1558-0210. DOI: 10.1109/TNSRE.2009.2033061.

[31] M. Saveriano and D. Lee, "Learning motion and impedance behaviors from human demonstrations," in *2014 11th International Conference on Ubiquitous Robots and Ambient Intelligence (URAI)*, 2014, pp. 368–373. DOI: 10.1109/URAI.2014.7057371.

[32] S. G. Hart and L. E. Staveland, "Development of NASA-TLX (Task Load Index): Results of Empirical and Theoretical Research," in *Advances in Psychology*, ser. Human Mental Workload, P. A. Hancock and N. Meshkati, Eds., vol. 52, North-Holland, Jan. 1988, pp. 139–183. DOI: 10.1016/S0166-4115(08)62386-9.

[33] A. Orhan, D. Verdel, O. Bruneau, F. Geffard, and B. Berret, "Combining Model-based and Data-based approaches for online predictions of human trajectories," in *IEEE RAS EMBS 10th International Conference on Biomedical Robotics and Biomechatronics (BioRob 2024)*, Heidelberg (Germany), France, Sep. 2024.

[34] A. Paraschos, C. Daniel, J. Peters, and G. Neumann, "Using probabilistic movement primitives in robotics," *Autonomous Robots*, vol. 42, no. 3, pp. 529–551, Mar. 2018, ISSN: 1573-7527. DOI: 10.1007/s10514-017-9648-7.

[35] P. Garrec, J. Friconneau, Y. Measson, and Y. Perrot, "ABLE, an innovative transparent exoskeleton for the upper-limb," in *2008 IEEE/RSJ International Conference on Intelligent Robots and Systems*, Nice: IEEE, Sep. 2008, pp. 1483–1488, ISBN: 978-1-4244-2057-5 978-1-4244-2058-2. DOI: 10.1109/IROS.2008.4651012.

[36] P. Garrec, "Screw and Cable Acutators (SCS) and Their Applications to Force Feedback Teleoperation, Exoskeleton and Anthropomorphic Robotics," in Feb. 2010, ISBN: 978-953-7619-78-7. DOI: 10.5772/7327.

[37] H. J. Hermens, B. Freriks, R. Merletti, *et al.*, "European Recommendations for Surface ElectroMyoGraphy," 1999.

[38] M. Patten, *Questionnaire Research: A Practical Guide*, 4th ed. New York: Routledge, Oct. 2016, ISBN: 978-1-315-26585-8. DOI: 10.4324/9781315265858.

[39] D. Verdel, A. Farr, T. Devienne, N. Vignais, B. Berret, and O. Bruneau, "Human movement modifications induced by different levels of transparency of an active upper limb exoskeleton," *Frontiers in Robotics and AI*, vol. 11, Jan. 2024, ISSN: 2296-9144. DOI: 10.3389/frobt.2024.1308958.

[40] S. S. Shapiro and M. B. Wilk, "An analysis of variance test for normality (complete samples)†," *Biometrika*, vol. 52, no. 3-4, pp. 591–611, Dec. 1965, ISSN: 0006-3444. DOI: 10.1093/biomet/52.3-4.591.

[41] S. H. Brown and J. D. Cooke, "Amplitude- and instruction-dependent modulation of movement-related electromyogram activity in humans," *The Journal of Physiology*, vol. 316, pp. 97–107, Jul. 1981, ISSN: 0022-3751. DOI: 10.1113/jphysiol.1981.sp013775.

[42] D. M. Corcos, G. L. Gottlieb, and G. C. Agarwal, "Organizing principles for single-joint movements. II. A speed-sensitive strategy," *Journal of Neurophysiology*, vol. 62, no. 2, pp. 358–368, Aug. 1989, ISSN: 0022-3077. DOI: 10.1152/jn.1989.62.2.358.

[43] G. Li, M. S. Shourijeh, D. Ao, C. Patten, and B. J. Fregly, "How Well Do Commonly Used Co-contraction Indices Approximate Lower Limb Joint Stiffness Trends During Gait for Individuals Post-stroke?" *Frontiers in Bioengineering and Biotechnology*, vol. 8, p. 588 908, 2020, ISSN: 2296-4185. DOI: 10.3389/fbioe.2020.588908.

[44] F. Just, Ö. Özen, S. Tortora, V. Klamroth-Marganska, R. Riener, and G. Rauter, "Human arm weight compensation in rehabilitation robotics: Efficacy of three distinct methods," *Journal of NeuroEngineering and Rehabilitation*, vol. 17, no. 1, p. 13, Feb. 2020, ISSN: 1743-0003. DOI: 10.1186/s12984-020-0644-3.

[45] D. Verdel, S. Bastide, F. Geffard, O. Bruneau, N. Vignais, and B. Berret, "Reoptimization of single-joint motor patterns to non-Earth gravity torques induced by a robotic exoskeleton," *iScience*, vol. 26, no. 11, Nov. 2023, ISSN: 2589-0042. DOI: 10.1016/j.isci.2023.108350.

[46] T. Başar and G. Olsder, "Dynamic Non-Cooperative Game Theory," vol. 160, Jan. 1999. DOI: 10.1137/1.9781611971132.

[47] Y. Li, G. Carboni, F. Gonzalez, D. Campolo, and E. Burdet, "Differential game theory for versatile physical human–robot interaction," *Nature Machine Intelligence*, vol. 1, no. 1, pp. 36–43, Jan. 2019, ISSN: 2522-5839. DOI: 10.1038/s42256-018-0010-3.

[48] H. Krebs, J. Palazzolo, L. Dipietro, *et al.*, "Rehabilitation Robotics: Performance-Based Progressive Robot-Assisted Therapy," *Autonomous Robots*, vol. 15, no. 1, pp. 7–20, Jul. 2003, ISSN: 1573-7527. DOI: 10.1023/A:1024494031121.

[49] Y. Mao and S. K. Agrawal, "Design of a Cable-Driven Arm Exoskeleton (CAREX) for Neural Rehabilitation," *IEEE Transactions on Robotics*, vol. 28, no. 4, pp. 922–931, Aug. 2012, ISSN: 1941-0468. DOI: 10.1109/TRO.2012.2189496.

[50] O. Dermy, A. Paraschos, M. Ewerton, J. Peters, F. Charpillet, and S. Ivaldi, "Prediction of Intention during Interaction with iCub with Probabilistic Movement Primitives," *Frontiers in Robotics and AI*, vol. 4, Oct. 2017, ISSN: 2296-9144. DOI: 10.3389/frobt.2017.00045.

[51] O. Dermy, F. Charpillet, and S. Ivaldi, "Multi-modal Intention Prediction with Probabilistic Movement Primitives," in *Human Friendly Robotics*, F. Ficuciello, F. Ruggiero, and A. Finzi, Eds., Cham: Springer International Publishing, 2019, pp. 181–196, ISBN: 978-3-319-89327-3. DOI: 10.1007/978-3-319-89327-3_14.